OUKA
The University of Osaka
Institutional Knowledge Archive

Title	Improving fatigue performance of fillet weld roots using soft metal insertion
Author(s)	Mao, Jiahao; Hirohata, Mikihito; Jiang, Feng et al.
Citation	Journal of Constructional Steel Research. 2025, 236, p. 110021
Version Type	VoR
URL	https://hdl.handle.net/11094/103293
rights	This article is licensed under a Creative Commons Attribution-NonCommercial-NoDerivatives 4.0 International License.
Note	

The University of Osaka Institutional Knowledge Archive : OUKA

https://ir.library.osaka-u.ac.jp/

The University of Osaka

Journal of Constructional Steel Research 236 (2026) 110021

Contents lists available at ScienceDirect

Journal of Constructional Steel Research

journal homepage: www.elsevier.com/locate/jcsr

Improving fatigue performance of fillet weld roots using soft metal insertion

Jiahao Mao [a], Mikihito Hirohata [a,*], Feng Jiang [a], Daichi Hamasaka [b]

[a] Graduate School of Engineering, The University of Osaka, Suita, Osaka 565-0871, Japan
[b] School of Engineering, The University of Osaka, Suita, Osaka 565-0871, Japan

ARTICLE INFO

Keywords:
Steel
Fillet weld root
Fatigue
Soft metal insertion
Bending–shear coupling

ABSTRACT

This study investigates the effect of soft metal insertion on the fatigue performance of fillet weld roots under bending-shear coupled loading. Previous research demonstrated that bonding-assisted welding improves fatigue strength, but issues such as epoxy combustion limited its application. To address this, zinc sheets were inserted between steel plates to establish zinc-steel bonding. Fatigue tests and numerical analyses were conducted on specimens with and without zinc insertion. Results indicate that zinc insertion significantly reduces fatigue stress at the weld root, extending fatigue life by approximately 70 % in some cases. However, the instability of zinc-steel bonding led to variations in fatigue strength among specimens. Finite element analysis using the effective notch stress (ENS) and equivalent displacement (ED) methods confirmed that zinc insertion reduces weld root stress and deformation by nearly 90 %. Both methods demonstrated similar accuracy in evaluating fatigue strength, but the ED method showed better alignment with the experimental results. This study demonstrates that zinc insertion effectively enhances the fatigue strength of fillet weld roots, providing a promising approach for improving welded joint durability.

1. Introduction

Steel is extensively utilized in engineering disciplines—including civil, mechanical, and structural engineering—due to its high tensile strength, ductility, and durability, which enable it to withstand large loads and deformations without failure [1,2]. Its relatively low production cost and high recyclability also contribute to its economic and environmental advantages [3,4]. In complex engineering structures such as bridges, buildings, and offshore platforms, steel plates are typically joined to form load-bearing frameworks using methods such as welding, riveting, or bolting, each selected based on performance requirements, accessibility, and anticipated loading conditions [5–8]. Among these, welding is widely adopted in civil and mechanical engineering due to its rapid construction, minimal weight addition, and aesthetically pleasing finish [9]. However, in civil engineering applications, steel plates are often thick, making non-penetration welded joints unavoidable [10,11]. Under the complex loading conditions of actual engineering applications, these non-penetration welded joints are often subjected to various types of cyclic loads, including Mode I (opening or tension), Mode II (in-plane shear), Mode III (out-of-plane shear), and their combinations [12,13]. The complex load conditions hinder the accurate fatigue assessment of such structural details. Furthermore, the structural characteristics of weld roots in these joints result in high stress concentrations, exacerbating the risk of fatigue failure. Studies indicate that such stress concentrations significantly shorten the lifespan of welded structures, necessitating frequent inspections and maintenance [14]. Moreover, fatigue cracks originating at the weld root are difficult to detect due to their internal location within the structure [11]. Addressing these challenges is critical for ensuring the structural integrity and longevity of welded steel components.

Numerous studies have explored solutions to weld root fatigue. Ahola et al. conducted experimental and numerical investigations on the fatigue strength of non-load-carrying transverse attachment joints with single-sided fillet welds, identifying the weld root as the critical fatigue failure mechanism. They examined fatigue life improvement techniques, such as curved plate edge shapes and varying weld penetration, which enhanced fatigue strength by up to 25 % in high-strength steel [15]. Raftar et al. evaluated various methods for assessing weld root fatigue strength in load-carrying fillet welds, including the nominal stress method, the effective notch stress (ENS) method, and the theory of critical distance. They also introduced the 4R method, an ENS-based approach incorporating the Smith-Watson-Topper mean stress

* Corresponding author at: 2-1, Yamada-oka, Suita, Osaka 565-0871, Japan.
E-mail address: hirohata@civil.eng.osaka-u.ac.jp (M. Hirohata).

https://doi.org/10.1016/j.jcsr.2025.110021
Received 8 February 2025; Received in revised form 22 September 2025; Accepted 28 September 2025
Available online 4 October 2025
0143-974X/© 2025 The Authors. Published by Elsevier Ltd. This is an open access article under the CC BY-NC-ND license (http://creativecommons.org/licenses/by-nc-nd/4.0/).

correction, and compared its accuracy to other assessment techniques [14]. Zhao et al. proposed a traction stress-based failure criterion to distinguish between weld toe and weld root failure in load-carrying cruciform fillet welds, addressing the challenge of predicting weld root failure [16].

In addition to the above explorations, studies have shown that bonding-assisted welded joints exhibit superior mechanical properties [17,18]. The authors previously attempted to enhance weld root fatigue life by inserting epoxy resin and heat-resistant rubber between steel plates. The bonding effect of epoxy on steel plates was utilized to reduce the cyclic tensile stress at the weld root, thereby improving fatigue life. However, during fabrication, it was observed that epoxy tended to burn during welding, compromising the welding quality. Even with the insertion of heat-resistant rubber, welding defects at the weld root could not be eliminated [19–21]. Consequently, this study investigates the use of soft metal insertion as an alternative bonding method. Soft metals such as zinc, aluminum, and copper offer superior high-temperature resistance and durability compared to epoxy [21,22]. Their use as a bonding material to assist welding can ensure better welding quality and provide a more durable bonding effect.

Previous studies have reported that fillet welds between bottom flanges and sole plates in steel bridge supports are susceptible to various types of fatigue cracks [23,24]. Among these, cracks initiating at the weld root have received relatively little attention due to the difficulty of detection, as illustrated in Fig. 1. These welds are typically subjected to bending–shear coupling. One of the challenges in evaluating the fatigue strength of such fillet welds is the difficulty in calculating nominal stress at the weld root, as these structural details are not covered in the IIW recommendations [25]. Therefore, this study focuses on the fillet welds around bridge supports, designing and conducting a series of experiments and numerical analyses to investigate the feasibility of bonding-assisted welding technology through soft metal insertion and its effectiveness in improving the fatigue performance of the weld root.

2. Experiments

2.1. Specimens

The specimens were designed based on actual bridge supports (Fig. 1), with dimensions scaled proportionally. Each specimen consisted of a 300 mm-long, 9 mm-thick flange plate and a 120 mm-long, 22 mm-thick sole plate joined by fillet welding (Fig. 2). The specimens were 40 mm wide. The length of the fillet weld leg was 4 mm. The specimens were divided into two categories, welding only (W) and zinc insertion (Z). In W specimens, the flange and bottom plates were joined solely by fillet welding, whereas in Z specimens, a 0.5 mm-thick zinc sheet was inserted between the steel plates to provide bonding. Additionally, W specimens were further divided into W0 (no gap) and W0.5 (0.5 mm gap) according to whether there was a gap between the flange plate and the bottom plate. The Z specimens were divided into Z0 (no distance), Z5 (5 mm distance) and Z10 (10 mm distance) according to the distance between the zinc sheet and the fillet weld root.

2.2. Fabrication

As shown in Fig. 3 (a), all specimens were initially fabricated from 200 mm-wide steel plates, which were surface-blasted before welding. For W0 specimens, the flange and sole plates were directly welded after surface treatment. For W0.5 specimens, a 0.5 mm-thick steel sheet was inserted between the flange plates and sole plates before welding. After welding, the steel sheet was removed to artificially create a 0.5 mm gap between the two steel plates. For Z specimens, a 0.5 mm-thick zinc sheet was inserted between the flange plates and sole plates before welding, and the zinc sheet was retained after welding (Fig. 3 (b)). The welding conditions were 130 A current, 18 V voltage, and 5.0 mm/s welding speed. During the welding process, the Z0 specimen had an insufficient distance between the zinc sheet and the weld root. The welding heat caused the zinc to vaporize, which negatively impacted the welding quality and posed a safety risk. The details of this issue will be discussed in Section 3.1. As a result, the Z0 specimen was excluded from subsequent tests. The remaining specimens underwent heat treatment in a high-temperature furnace, where they were heated to 500 °C over 8 h, held at 500 °C for an additional 8 h, and then slowly cooled to room temperature in the furnace (Fig. 3 (c)). The heat treatment aimed to melt the zinc sheet, of which the melting temperature was around 420 °C, allowing it to better fill the gap between the steel plates and enhance the zinc-steel bond. According to previous studies, steel exhibits significant creep only above 550 °C, and metallurgical changes typically require even higher temperatures [26–28]. Therefore, it can be considered that this heat treatment did not affect the steel properties in the specimens. After heat treatment, all specimens were cut to a final width of 40 mm for subsequent fatigue testing (Fig. 3 (d)). Previous studies have pointed out that residual stress is partially released during cutting. Specifically, the longitudinal residual stress of the entire specimen and transverse residual stress on the cut surface are almost fully released, while a low level of transverse residual stress remains internally [29]. Considering that the residual stress at the fatigue crack observation surface is nearly eliminated, and the internal residual stress is similarly low across all specimens, its limited influence was neglected in the subsequent analysis.

2.3. Materials

To investigate the fatigue performance of fillet welds near bridge supports, a commonly used structural steel in Japan, SM400A [30], was selected for the specimens. The specimens consisted of two steel plate thicknesses: 9 mm and 22 mm. The welding wire used was G49A0C12 in JIS Z 3312, classified as a 490 N/mm^2 welding material [31]. The composition ratios and mechanical properties of these steels are provided in Table 1 and Table 2, respectively. To explore the feasibility of bonding-assisted welding through soft metal in preventing root fatigue cracks and increasing fatigue life, zinc was chosen as the insert material due to its low cost and good corrosion resistance compared to other soft metals. Moreover, zinc has a relatively low melting point (approximately 420 °C), which minimizes thermal effects on the steel plates during heating. The zinc sheets inserted between the steel plates were made of pure zinc, and their mechanical properties are also shown in

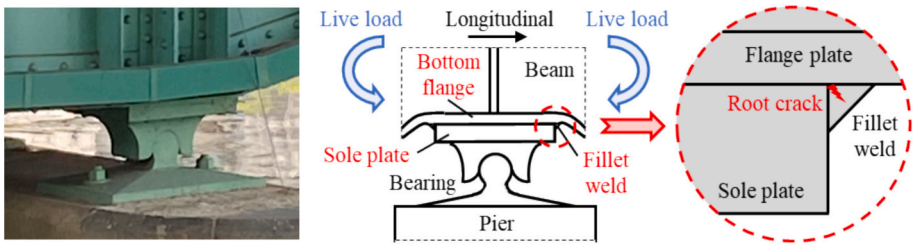

Fig. 1. Weld root fatigue problem of steel bridge supports.

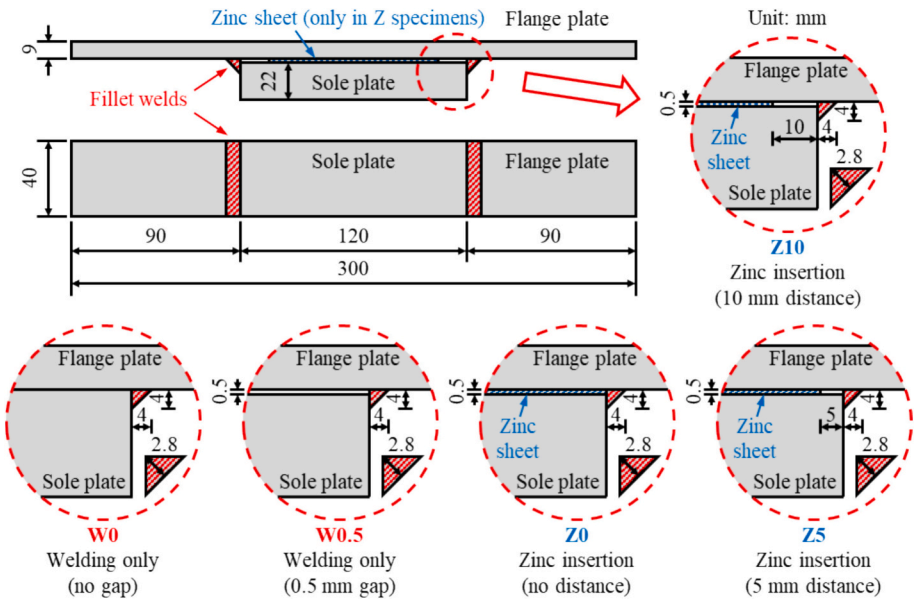

Fig. 2. Details of the specimens (unit: mm).

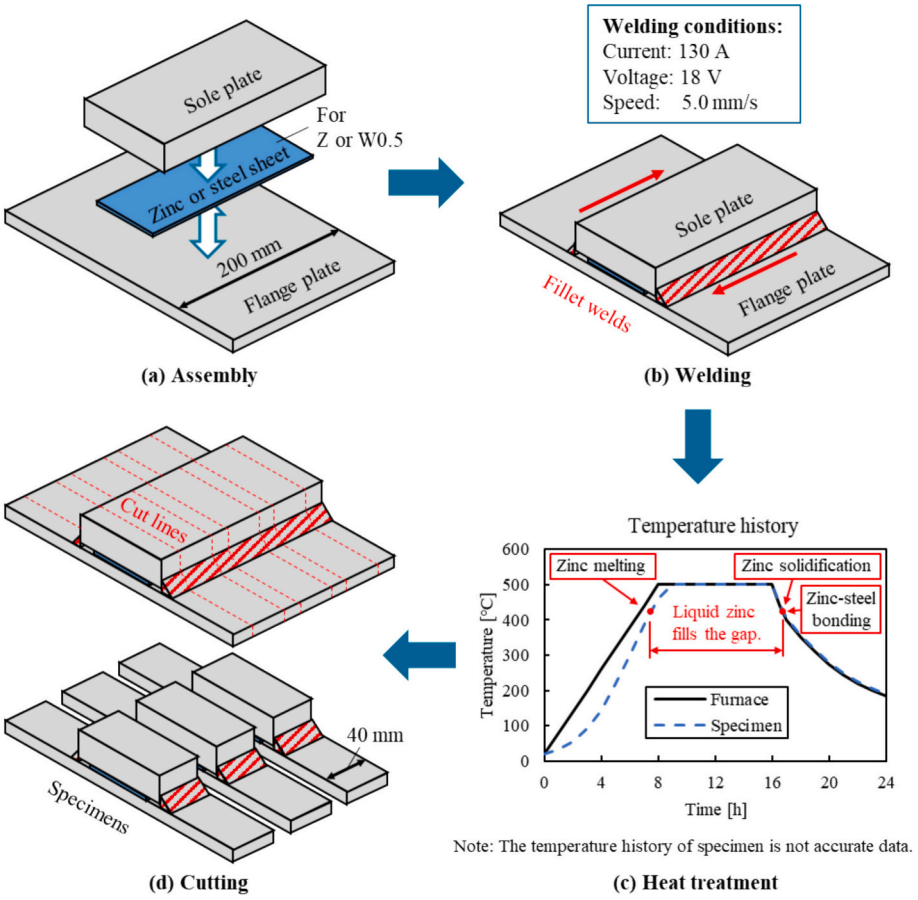

Fig. 3. Fabrication process of the specimens.

Table 2.

The zinc-steel bonding strength was tested by the specimen shown in Fig. 4. The specimen consisted of two steel blocks sandwiching a 0.5 mm-thick zinc sheet and had dimensions of 40 mm × 40 mm × 44.5 mm. It was heated for the same duration as the fatigue specimen to establish the zinc-steel bond. The bonding strength was then tested through an axial tensile test (Fig. 5). A total of five specimens were tested, yielding an average strength of 0.92 N/mm^2.

2.4. Test setup and measurements

As shown in Fig. 6, a four-point bending loading mode was chosen to

Table 1
Composition ratios of steels.

Category	Composition ratios [mass %]				
	C	Si	Mn	P	S
SM400A (9 mm)	0.08	0.25	0.82	0.018	0.003
SM400A (22 mm)	0.07	0.20	0.84	0.016	0.007
G49A0C12	0.09	0.44	0.94	0.012	0.012

Note: The data for G49A0C12 are nominal values.

Table 2
Mechanical properties of metals.

Category	Elastic modulus [N/mm^2]	Yield strength [N/mm^2]	Tensile strength [N/mm^2]	Elongation [%]
SM400A (9 mm)	2.06×10^5	293	447	31
SM400A (22 mm)	2.06×10^5	285	439	34
G49A0C12	2.06×10^5	460	540	–
Zinc sheet	1.18×10^5	–	118	–

Note: The data for G49A0C12 and the zinc sheet are nominal values. All elastic moduli are nominal values.

simulate the bending-shear coupled loading of fillet welds between the bottom flange and sole plate of bridge supports during the fatigue tests. The tests were carried out using a servo-hydraulic fatigue test machine with a cyclic load ratio (minimum load / maximum load) of 0.1 and a frequency of 5 Hz. After excluding all Z0 specimens and other specimens with poor welding quality, a total of 25 specimens were tested, consisting of three W0 specimens, eight W0.5 specimens, six Z5 specimens, and eight Z10 specimens. During the fatigue tests, the generation and development of fatigue cracks at the weld root were monitored using fluorescent magnetic particle inspection, as shown in Fig. 7. The fatigue life was defined as the number of load cycles until a fatigue crack longer than 0.2 mm developed at the weld root. If no fatigue failure was observed after two million cycles, the test was terminated.

3. Experimental results

3.1. Welding quality

Previous studies on epoxy resin bonding-assisted welding technology reported problems with unstable weld quality and defects, such as incomplete root penetration and incomplete epoxy filling [21,32]. These problems arise primarily from the difficulty in precisely controlling the volume of epoxy applied. In contrast, these defects did not occur in soft metal bonding-assisted welding using zinc, due to the better controllability of the insertion volume. However, due to the proximity of the zinc sheet to the weld bead, welding failures were common in the Z0 specimens, while the Z5 and Z10 specimens exhibited good welding quality. Fig. 8 presents macrographs of the welds in W0.5, Z0, Z5, and Z10 specimens. The physical properties of zinc, including its lower specific heat capacity and higher thermal conductivity compared to steel, as well as its significantly lower boiling point than steel's melting point, led to zinc vaporization when placed too close to the weld. As a result, excessive heat input during welding caused spattering in Z0 specimens, compromising weld quality and posing safety risks. In contrast, the Z5 and Z10 specimens maintained a safe distance from the weld, preventing

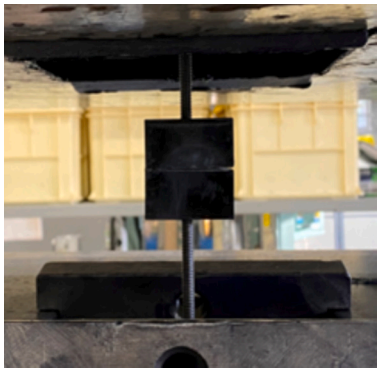

Fig. 5. Axial tensile test setup.

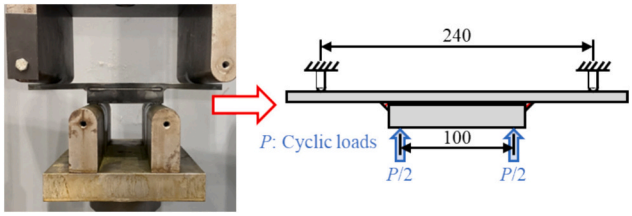

Fig. 6. Fatigue test setup (unit: mm).

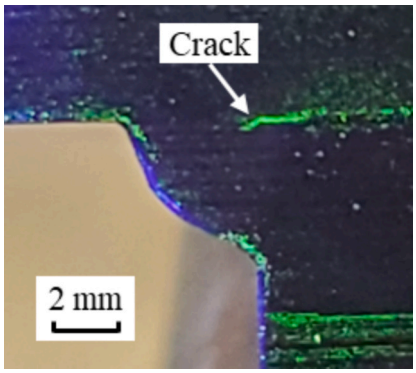

Fig. 7. Root fatigue crack.

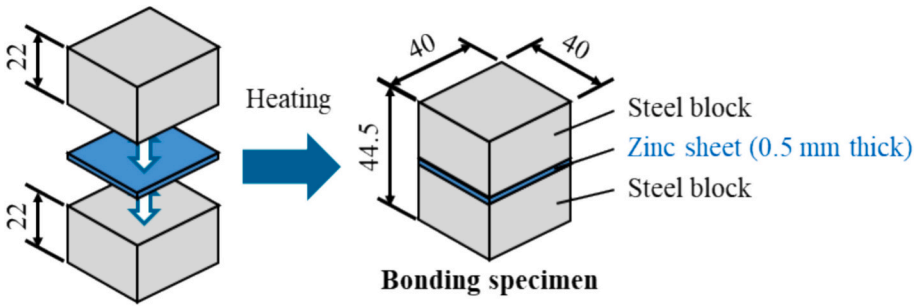

Fig. 4. Details of the zinc-steel bonding specimen (unit: mm).

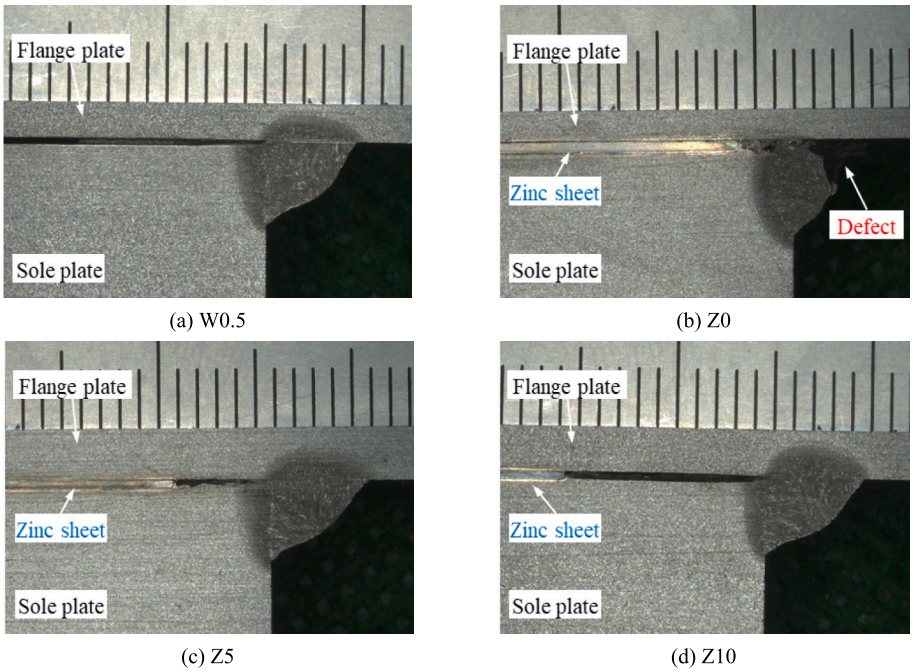

Fig. 8. Macrographs around the welds.

zinc vaporization and achieving welding quality comparable to that of W0.5 specimens. These findings suggest that when applying soft metal bonding-assisted welding, key material properties such as melting point, boiling point, specific heat capacity, and thermal conductivity should be carefully considered to avoid welding defects and hazards. Maintaining a sufficient safety distance between the soft metal insert and the weld is recommended to ensure optimal welding quality.

3.2. Fatigue life

The nominal stress at the root of fillet welds subjected to bending–shear coupling, such as those near bridge supports, is difficult to calculate accurately. Previous study has attempted to evaluate weld root fatigue strength using nominal stress at weld roots but achieved limited accuracy [21]. Therefore, this study adopts an alternative approach by analyzing the S—N relationship using the nominal stress at the bottom flange (Fig. 9), which is easier for calculation. Excluding those exceeding two million cycles, the remaining data points form two distinct linear trends in a double logarithmic coordinate system. The blue line is fitted by some Z specimens, and the red line is fitted by the W specimen and the remaining Z specimens. More than half of the Z specimens exhibited significantly higher fatigue strength, demonstrating a fatigue life comparable to W specimens under a load range more than 1.7 times that of W specimens. However, other Z specimens showed no significant difference from W specimens, likely due to variations in zinc-steel bonding strength, which will be discussed in Section 3.3. In addition, W0 specimens exhibited slightly lower fatigue strength than W0.5 specimens, potentially due to a sharper weld root in W0 specimens, leading to greater stress concentration. This hypothesis will be further verified through finite element analysis.

3.3. Zinc-steel bonding strength

A total of five zinc-steel bonding specimens were tested, and the results are presented in Fig. 10. All specimens failed within the zinc sheet, with a layer of zinc remaining firmly adhered to the bonding interfaces of the steel blocks on both sides, as illustrated in Fig. 10 (b). This suggests that the zinc–steel bonding strength appears to exceed the

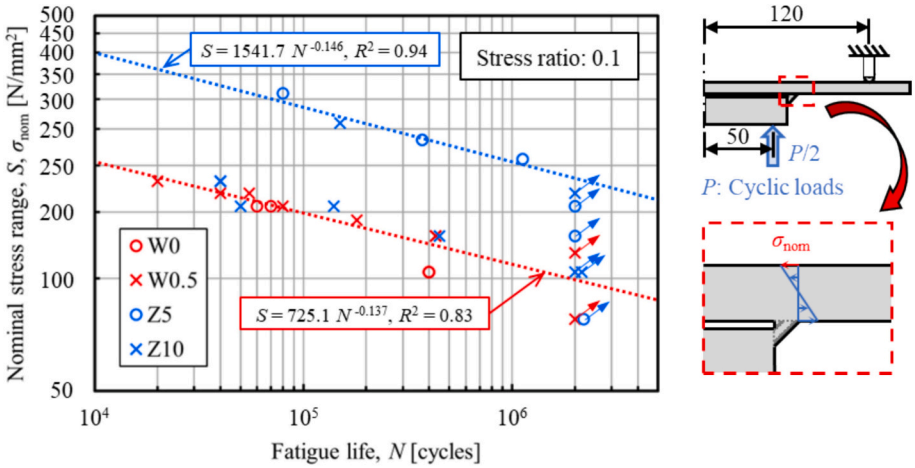

Fig. 9. *S*—*N* relationship (nominal stress).

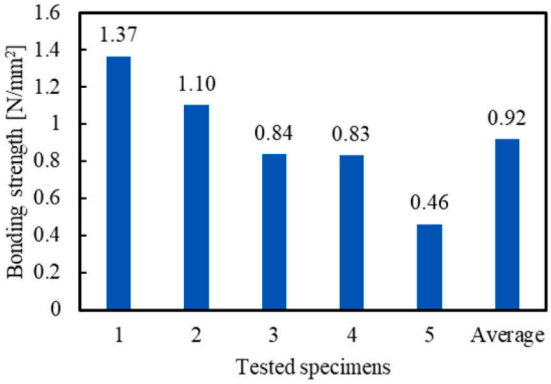

(a) Bonding strength

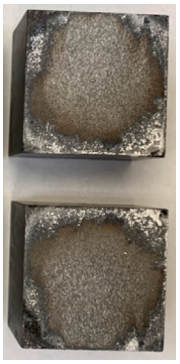

(b) Failed bonding specimen

Fig. 10. Zinc-steel bonding test results.

strength of the zinc sheet. However, numerous fine internal defects formed during the liquefaction and solidification of zinc, resulting in a significant decrease in its strength. The average bonding strength of the five specimens was measured to be 0.92 N/mm^2, but significant variation was observed among the specimens, leading to differences in the fatigue strength of the Z specimens. Z specimens with higher zinc-steel bonding strength exhibited greater weld root fatigue resistance, as their bonding provided a more sustained effect in reducing fatigue stress at the weld root. Conversely, Z specimens with lower zinc-steel bonding strength likely experienced premature bond failure, preventing effective stress reduction at the weld root. As a result, these specimens displayed fatigue performance similar to that of W specimens. The zinc-steel bond extends the fatigue life of the weld root through a self-sacrificial mechanism, which will be further analyzed in conjunction with finite element analysis.

4. Numerical analyses

For fillet welds subjected to bending–shear coupling, such as those near bridge supports, the inability to directly calculate the nominal stress at the weld root complicates fatigue strength evaluation [21]. The IIW recommendations do not involve the calculation case of nominal stress for such structural details [25]. Even with finite element analysis, weld root stress singularity remains a challenge, as the theoretical stress at the singularity tends toward infinity. Therefore, the stress magnitude at the weld root is highly sensitive to element size [33]. To address this issue, two methods have been proposed in previous studies, namely the effective notch stress (ENS) method and the equivalent displacement (ED) method. In this study, a series of finite element models were developed using both the ENS and ED methods to evaluate the fatigue strength of these fillet welds and assess the effectiveness of soft metal bonding-assisted welding with zinc.

4.1. Effective notch stress

The ENS method is proposed by Fricke et al. based on the microstructural support effect proposed by Neuber [34,35]. This approach mitigates stress singularity by introducing an artificial notch at the weld root, allowing for the obtained stress to be averaged near the notch [36,37]. As shown in Fig. 11, this method artificially introduces a standardized keyhole or U-shaped notch, or applies a smooth transition at the stress singularity in the finite element model. The fatigue stress is then reflected by the maximum principal stress or von Mises stress distributed on the notch circumference. Currently, there are two commonly used notch reference radii: $r_{ref} = 1$ mm and $r_{ref} = 0.05$ mm, which are suitable for plate thickness ≥ 5 mm and < 5 mm, respectively [38]. This distinction prevents the artificial notch from affecting the stress distribution, which could otherwise cause misestimation of fatigue strength. In addition, it is recommended that the element size on the notch circumference should not be greater than r_{ref} / 4 [39]. The ENS method is widely utilized, due to its compatibility with conventional stress-based fatigue criterion and its accessibility through elastic finite element analysis. However, it also increases the complexity of modeling and meshing, especially for high-precision, three-dimensional finite element models.

4.2. Equivalent displacement

The ED method, first proposed by Tateishi et al., evaluates structural fatigue performance under both Mode I and Mode II loading (bending-shear coupling) in fracture mechanics [40]. As shown in Fig. 12, this method establishes a finite element model based on the actual configuration and selects four specific nodes near the weld root. The displacement components of these nodes in the x- and y-directions are extracted from the finite element analysis, and the displacement components u and v are then calculated respectively using the following

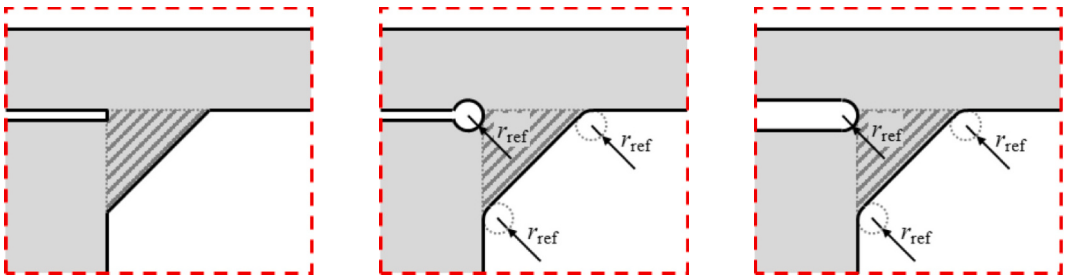

(a) Ideal (b) Keyhole notch (c) U-shaped notch

Fig. 11. Artificial notch in finite element models.

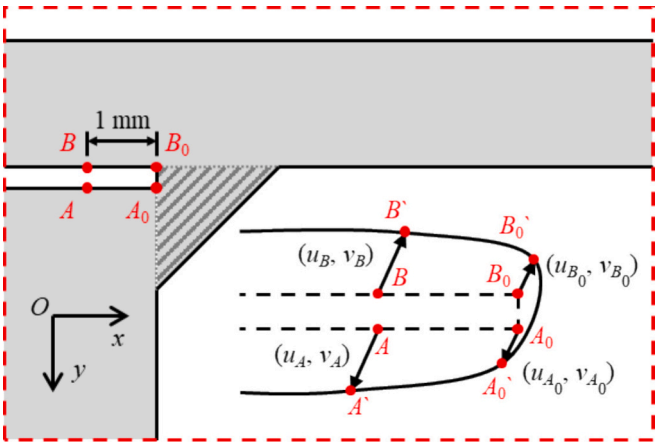

Fig. 12. Node displacements near the weld root.

equations:

$$u = |(u_A - u_{A0}) - (u_B - u_{B0})| \tag{1}$$

$$v = |(v_A - v_{A0}) - (v_B - v_{B0})| \tag{2}$$

where, u_A, u_{A0}, u_B, and u_{B0} are the displacements of nodes A, A_0, B, and B_0 in the x-direction, respectively; and v_A, v_{A0}, v_B, and v_{B0} are their displacements in the y-direction, respectively.

The displacement components u and v correspond to Mode II and Mode I loading, respectively. The equivalent displacement d is then determined using the following equation:

$$d = \sqrt{3u^2 + v^2} \tag{3}$$

This method leverages the low sensitivity of displacement to element size, offering a different solution to the stress singularity issue [40]. Although less commonly used, the ED method presents advantages such as simplified modeling and reduced element refinement requirements, making it a promising approach for future applications. However, as it relies on a displacement-based criterion, it is not well compatible with the currently widely used stress-based criterion. Consequently, further experimental validation and numerical studies are necessary to establish the method's effectiveness and reliability.

4.3. Finite element models

Both the ENS and ED methods rely on elastic finite element analysis. Therefore, 3D elastic finite element models were developed in ABAQUS. To enhance computational efficiency, the 1/4 models were used based on symmetry. The basic geometric dimensions match those of the specimens in Fig. 2, with local modifications near the weld root, as shown in Fig. 13. For the ENS models, because the plate thickness exceeded 5 mm, a notch of r_{ref} = 1 mm was adopted. The minimum element size on the notch perimeter is 0.2 mm, transitioning to the global mesh, with a maximum element size of 1 mm. For ED models, the gap between the bottom flange and sole plate is simplified as a rectangle, with a 0.1 mm element size near the weld root, also transitioning to a 1 mm global mesh. All models use 8-node hexahedral solid elements with reduced integration (C3D8R). Monotonic loading is applied, with load amplitudes corresponding to specimen load ranges. The base and weld materials are assumed to have identical properties, with elastic moduli for steel and zinc listed in Table 2 and Poisson's ratios set at 0.3. The zinc sheet was modeled as solid elements tied rigidly to the adjacent steel surfaces to simulate bonding, assuming ideal bonding without failure. Since welding residual stresses were partially released when the specimens were cut, their influence is neglected in the analysis.

4.4. Comparison and discussion

The four groups of specimens (W0, W0.5, Z5 and Z10) were evaluated by the ENS and ED methods with a load range of 3 kN, corresponding to a σ_{nom} of approximately 155.6 N/mm^2 (Fig. 9). The maximum principal stress distributions near the weld root from the ENS and ED models are shown in Fig. 14 and Fig. 15, respectively. All W specimens exhibited severe stress concentrations at the weld root, whereas the Z specimens, which incorporated zinc insertion, showed a marked reduction in stress. The ENS and ED results of each model are summarized in Fig. 16. The two methods respectively demonstrated that

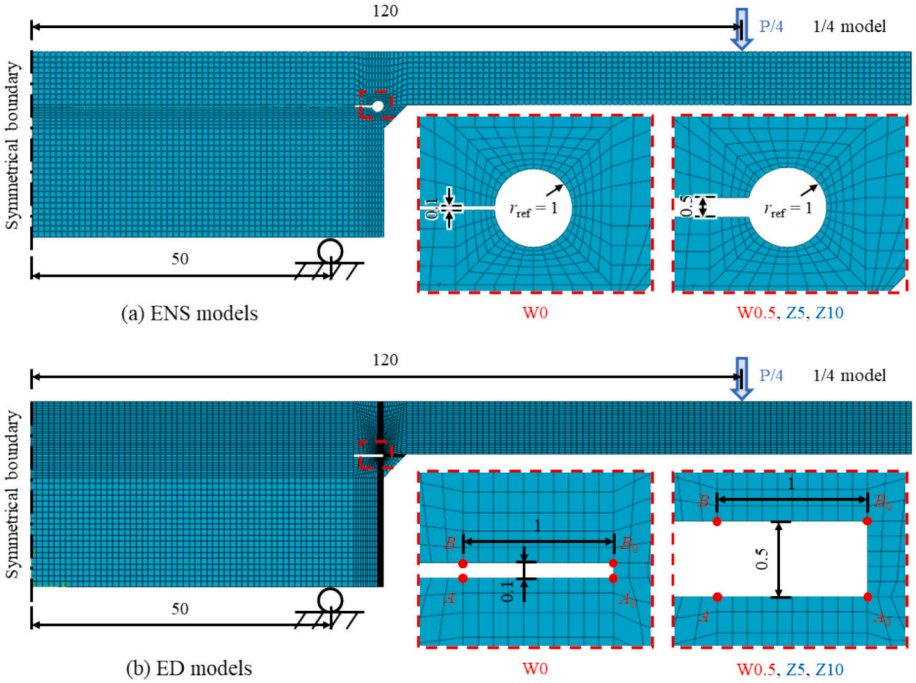

Fig. 13. Finite element models (unit: mm).

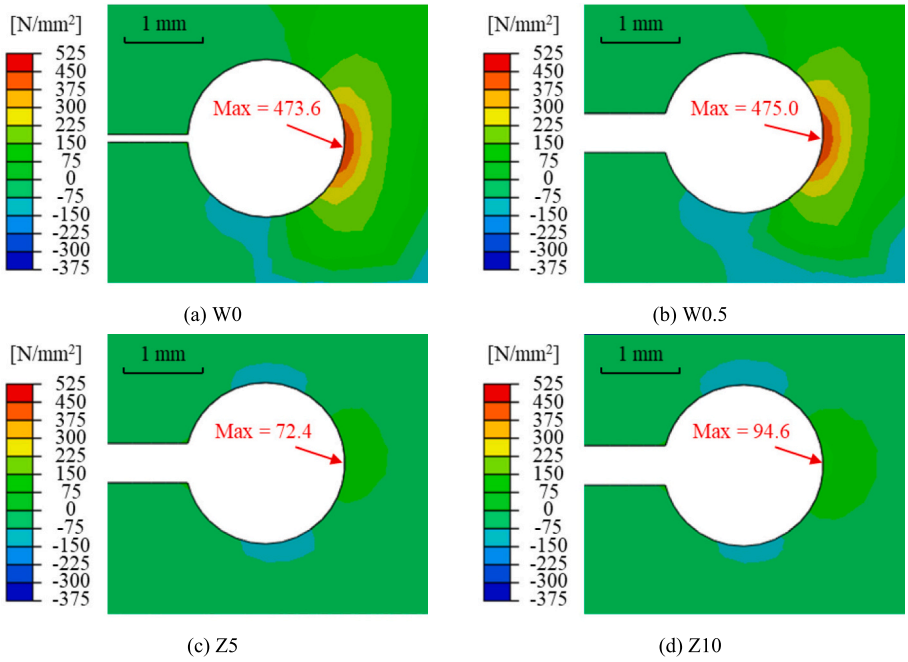

Fig. 14. Maximum principal stress distributions of the ENS models.

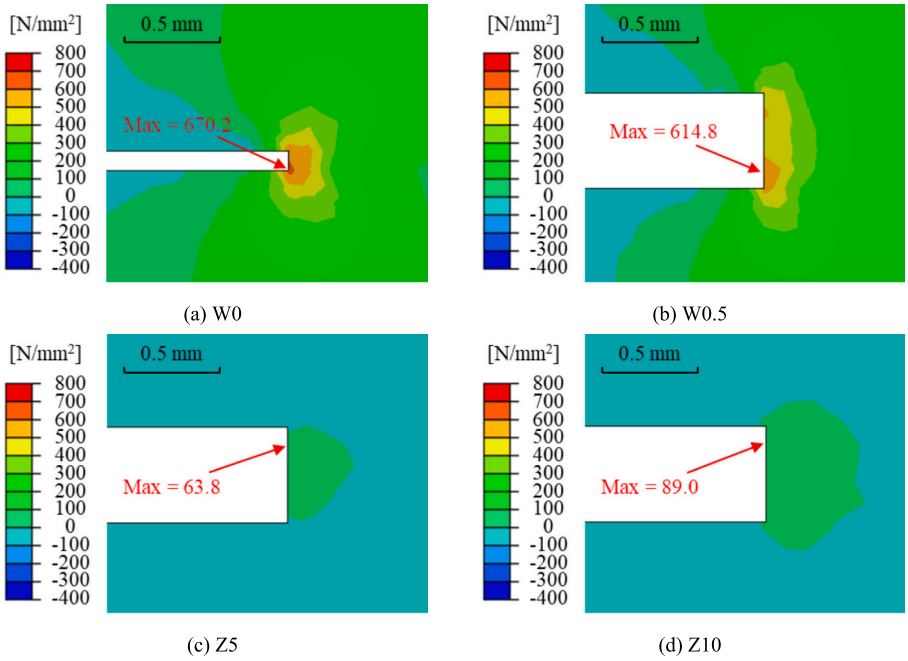

Fig. 15. Maximum principal stress distributions of the ED models.

the insertion of zinc can significantly reduce the stress and deformation of the weld root, with the results for the Z models being approximately 10 %–20 % of those for the W models. This highlights the effectiveness of inserting zinc sheets between the bottom flange and sole plate to create zinc-steel bonding, which helps prevent fatigue cracks at the weld root. However, not all Z specimens showed a significant improvement in fatigue strength, with the increase ratio being around 70 %. This could be attributed to the instability and low strength of the zinc-steel bonding. Under cyclic load, the zinc-steel bonding fails before the fatigue cracks at the weld root appear, thus prolonging the weld root's fatigue life by sacrificing itself. Therefore, for the Z specimens with higher zinc-steel bonding strength, the fatigue failure of the weld root can be divided into two stages: before and after the zinc-steel bonding failure. It is assumed that the specimens conform to the cumulative fatigue damage rule. Before the failure of the zinc-steel bonding, the fatigue stress at the weld root is below 20 % of the stress after bonding failure, so the accumulated fatigue damage can be considered negligible. According to the fitted trend line in Fig. 9, it can be inferred that the stage before the failure of zinc-steel bonding accounts for more than 95 % of the total fatigue life of these specimens.

In the *S*—*N* relationship (nominal stress) shown in Fig. 9, the fatigue strength of the W0 specimens is similar to that of the W0.5 specimens, with only a slight decrease for the W0 specimens. Both the ENS and ED models show nearly identical results for the W0 and W0.5 specimens.

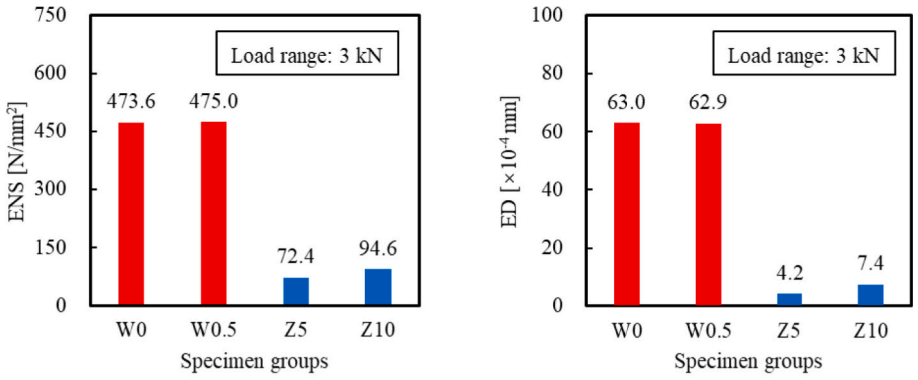

(a) ENS method (b) ED method

Fig. 16. Effect of zinc insertion on improving fatigue strength.

However, it is noteworthy that the ENS for the W0 model is smaller than that for the W0.5 model, which exhibits a trend opposite to the experimental results. In contrast, the ED results for the W0 and W0.5 models are also nearly identical, and their trend aligns with the experimental data. Therefore, the ED method appears to offer a more accurate evaluation, though additional data is needed for further validation. Subsequently, the fatigue strength of all W specimens was evaluated using both the ENS and ED methods, resulting in the *S*—*N* relationship (ENS) and *D*—*N* relationship shown in Fig. 17. The fatigue life data were extracted from the experimental results. Excluding specimens that did not develop fatigue cracks after more than 2 million cycles, the remaining specimens were fitted. The correlation coefficients of the trend lines fitted to the *S*—*N* relationship (ENS) and *D*—*N* relationship were approximately 0.87 and 0.88, respectively, indicating similar evaluation accuracy for both methods. However, the ED method proves more convenient for modeling, suggesting its potential for broader application. Similar findings have been reported where displacement-based criteria may outperform stress-based criteria in specific fatigue assessments [41].

5. Conclusions

This study proposes a method for inserting zinc between two steel plates to establish zinc-steel bonding, thereby improving the fatigue performance of the weld root in a fillet weld subjected to bending-shear coupled loads. The effectiveness of this method was investigated through experimental and simulation analyses, leading to the following conclusions:

(1) In bonding-assisted welding, inserting zinc between steel plates produces a more stable and higher-quality fillet weld than inserting epoxy resin, owing to the improved control over the volume of soft metal inserted. It is important to ensure a safety distance ($\geq$ 5 mm) between the inserted soft metal sheet and the weld root.

(2) Establishing zinc-steel bonding improves the fatigue strength of the weld root under bending-shear coupled loads by approximately 70 %. However, due to the instability of zinc-steel bonding strength, some zinc-inserted specimens (Z) still exhibit fatigue strength similar to that of the welding-only specimens (W).

(3) Both the effective notch stress (ENS) method and the equivalent displacement (ED) method demonstrate that zinc insertion significantly improves the fatigue strength of the weld root. When the zinc-steel bonding takes effect, the fatigue stress and deformation of the weld root in the Z specimens are reduced to about 10 %–20 % of those in the W specimens. This demonstrates the potential of bonding-assisted welding using zinc in improving the fatigue strength of the fillet weld root.

(4) For evaluating the fatigue strength of fillet weld roots with varying welding gaps, both the ENS and ED methods showed similar accuracy. However, the ED method more consistently aligned with the trend of the experimental results.

Given the observed instability in zinc-steel bonding in this study, more research needs to be performed on developing methods to establish more stable and higher-strength zinc-steel bonding, which will help promote the application of this method in engineering.

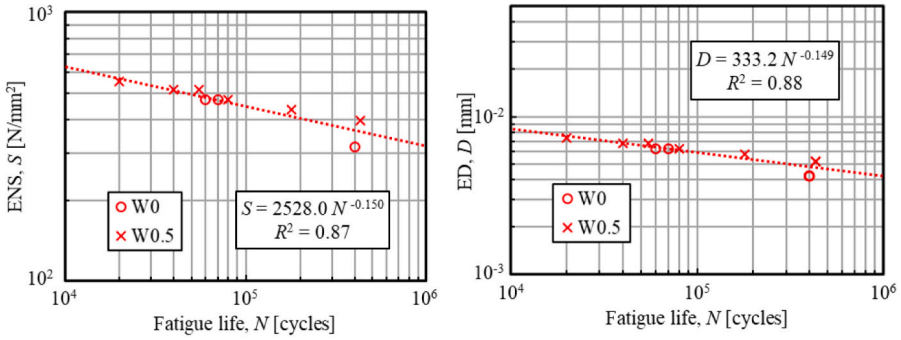

(a) *S*-*N* relationship (ENS) (b) *D*-*N* relationship

Fig. 17. Comparison of fatigue life evaluations for the W specimens.

CRediT authorship contribution statement

Jiahao Mao: Writing – review & editing, Writing – original draft, Visualization, Validation, Software, Methodology, Investigation, Formal analysis, Data curation, Conceptualization. **Mikihito Hirohata:** Writing – review & editing, Supervision, Resources, Project administration, Funding acquisition, Data curation, Conceptualization. **Feng Jiang:** Writing – review & editing, Visualization, Investigation, Formal analysis. **Daichi Hamasaka:** Validation, Methodology, Investigation, Data curation.

Declaration of competing interest

The authors declare that there are no known conflicts of interest associated with this publication.

We confirm that the manuscript has been read and approved by all named authors and that there are no other persons who satisfied the criteria for authorship but are not listed. We further confirm that the order of authors listed in the manuscript has been approved by all of us.

Acknowledgments

Partial financial support for this research was provided by a grant from the Japan Iron and Steel Federation (JISF) for steel structure research and education 2023 and 2024, for which we are very grateful.

Data availability

The data that has been used is confidential.

References

[1] P. Soroushian, K.B. Choi, Steel mechanical properties at different strain rates, J. Struct. Eng. 113 (4) (1987) 663–672, https://doi.org/10.1061/(ASCE)0733-9445(1987)113:4(663).
[2] X. Qiang, F. Bijlaard, H. Kolstein, Dependence of mechanical properties of high strength steel S690 on elevated temperatures, Constr. Build. Mater. 30 (2012) 73–79, https://doi.org/10.1016/j.conbuildmat.2011.12.018.
[3] X. Cheng, X. Zhao, Y. Chen, Z. Li, A model study on affordable steel residential housing in China, Front. Struct. Civ. Eng. 6 (2012) 288–296, https://doi.org/10.1007/s11709-012-0171-9.
[4] X. Zhang, S. Zhao, Z. Liu, F. Wang, Utilization of steel slag in ultra-high performance concrete with enhanced eco-friendliness, Constr. Build. Mater. 214 (2019) 28–36, https://doi.org/10.1016/j.conbuildmat.2019.04.106.
[5] D.H. Phillips, Welding Engineering: An Introduction, John Wiley & Sons, 2023.
[6] J. Wu, C. Chen, Y. Ouyang, D. Qin, H. Li, Recent development of the novel riveting processes, Int. J. Adv. Manuf. Technol. 117 (2021) 19–47, https://doi.org/10.1007/s00170-021-07689-w.
[7] A.M. De Jesus, A.L. da Silva, J.A. Correia, Fatigue of riveted and bolted joints made of puddle iron—a numerical approach, J. Constr. Steel Res. 102 (2014) 164–177, https://doi.org/10.1016/j.jcsr.2014.06.012.
[8] M. Amer, Y. Du, Z. Chen, S.A. Laqsum, Y. Zhang, Seismic behavior of concrete-filled steel tubes column frame-buckling restrained steel plate shear walls connected with bolt/weld, Thin-Walled Struct. 189 (2023) 110911, https://doi.org/10.1016/j.tws.2023.110911.
[9] M. Tümer, C. Schneider-Bröskamp, N. Enzinger, Fusion welding of ultra-high strength structural steels–a review, J. Manuf. Process. 82 (2022) 203–229, https://doi.org/10.1016/j.jmapro.2022.07.049.
[10] H. Zhao, X. Li, S.T. Lie, Fracture analysis of load-carrying cruciform welded joint with a surface crack at weld toe, Eng. Fract. Mech. 241 (2021) 107393, https://doi.org/10.1016/j.engfracmech.2020.107393.
[11] Y. Peng, Z. Dai, J. Chen, X. Ju, J. Dong, Fatigue behaviour of load-carrying fillet-welded cruciform joints of austenitic stainless steel, J. Constr. Steel Res. 184 (2021) 106798, https://doi.org/10.1016/j.jcsr.2021.106798.
[12] Y. Murakami, Y. Fukushima, K. Toyama, S. Matsuoka, Fatigue crack path and threshold in mode II and mode III loadings, Eng. Fract. Mech. 75 (3–4) (2008) 306–318, https://doi.org/10.1016/j.engfracmech.2007.01.030.
[13] Y. Wang, W. Wang, B. Zhang, C.Q. Li, A review on mixed mode fracture of metals, Eng. Fract. Mech. 235 (2020) 107126, https://doi.org/10.1016/j.engfracmech.2020.107126.
[14] H.R. Raftar, E. Dabiri, A. Ahola, T. Björk, Weld root fatigue assessment of load-carrying fillet welded joints: 4R method compared to other methods, Int. J. Fatigue 156 (2022) 106623, https://doi.org/10.1016/j.ijfatigue.2021.106623.
[15] A. Ahola, T. Skriko, K. Lipiäinen, T. Björk, On the weld root fatigue strength and improvement techniques for non-load-carrying transverse attachment joints with single-sided fillet welds and made of mild and ultra-high-strength steels, Eng. Struct. 249 (2021) 113373, https://doi.org/10.1016/j.engstruct.2021.113373.
[16] Z. Zhao, T. Zhang, W. Song, W. Jiang, P. Wang, S. Xing, X. Pei, A data-driven analysis for fatigue failure mode identification in load-carrying fillet welded joint with mechanical data augmentation, Fatigue Fract. Eng. Mater. Struct. 45 (11) (2022) 3418–3435, https://doi.org/10.1111/ffe.13811.
[17] M. Hirohata, Static tensile strength characteristics of fillet welding lap joints assisted with bonding, Weld. Int. 30 (1) (2016) 9–17, https://doi.org/10.1080/09507116.2014.921085.
[18] T. Nonnenmann, R. Beygi, R.J. Carbas, L.F. da Silva, A. Öchsner, Synergetic effect of adhesive bonding and welding on fracture load in hybrid joints, J. Adv. Joining Processes 6 (2022) 100122, https://doi.org/10.1016/j.jajp.2022.100122.
[19] H. Mikihito, I. Yoshito, Fatigue characteristics of patch plate joints by fillet welding assisted with bonding, Weld. Int. 32 (4) (2018) 243–253, https://doi.org/10.1080/09507116.2017.1346217.
[20] Y. Xu, M. Hirohata, T. Suzuki, H. Konishi, S. Tominaga, Assistive bonding assisted prevention of weld root fatigue cracks, Welding Lett. 40 (4) (2022) 5WL–8WL, https://doi.org/10.2207/qjjws.40.5WL.
[21] J. Mao, M. Hirohata, Y. Xu, K. Chang, Fatigue performance of bonding-assisted fillet weld roots by inserting adhesive material, Fatigue Fract. Eng. Mater. Struct. 47 (10) (2024) 3646–3657, https://doi.org/10.1111/ffe.14400.
[22] H. Warlimont, W. Martienssen (Eds.), Springer Handbook of Materials Data, Springer, 2018.
[23] K. Tateishi, T. Natori, C. Miki, Fatigue damage of shoes in plate girder bridges and improvement of their details, J. JSCE 1994 (489) (1994) 167–176 (in Japanese), https://doi.org/10.2208/jscej.1994.489_167.
[24] G. Alencar, A. de Jesus, J.G.S. da Silva, R. Calçada, Fatigue cracking of welded railway bridges: a review, Eng. Fail. Anal. 104 (2019) 154–176, https://doi.org/10.1016/j.engfailanal.2019.05.037.
[25] A.F. Hobbacher, Recommendations for Fatigue Design of Welded Joints and Components vol. 47, Springer International Publishing, Cham, 2016.
[26] T.Z. Harmathy, A comprehensive creep model, ASME. J. Basic Eng. 89 (3) (1967) 496–502, https://doi.org/10.1115/1.3609648.
[27] H. Colpaert, Metallography of Steels: Interpretation of Structure and the Effects of Processing, Asm International, 2018.
[28] M.P. Aung, H. Katsuda, M. Hirohata, Fatigue-performance improvement of patch-plate welding via PWHT with induction heating, J. Constr. Steel Res. 160 (2019) 280–288, https://doi.org/10.1016/j.jcsr.2019.05.047.
[29] H. Liang, Y. Kan, H. Chen, R. Zhan, X. Liu, D. Wang, Effect of cutting process on the residual stress and fatigue life of the welded joint treated by ultrasonic impact treatment, Int. J. Fatigue 143 (2021) 105998, https://doi.org/10.1016/j.ijfatigue.2020.105998.
[30] Japanese Industrial Standards Committee, Rolled steels for welded structure, JIS G 3106 (2017) 2017 (in Japanese).
[31] Japanese Industrial Standards Committee, Solid wires for MAG and MIG welding of mild steel, high strength steel and low temperature service steel, JIS Z 3312 (2009) 2009 (in Japanese).
[32] International Organization for Standardization, Welding - Fusion-Welded Joints in Steel, Nickel, Titanium and Their Alloys (Beam Welding Excluded) - Quality Levels for Imperfections, Fourth edition, 2023, p. 2023. ISO 5817.
[33] H. Bartsch, S. Citarelli, M. Feldmann, Generalisation of the effective notch stress concept for the fatigue assessment of arbitrary steel structures, J. Constr. Steel Res. 201 (2023) 107715, https://doi.org/10.1016/j.jcsr.2022.107715.
[34] W. Fricke, Guideline for the fatigue assessment by notch stress analysis for welded structures, Int. Inst. Welding 13 (2008) 2208–2240.
[35] W. Fricke, IIW Recommendations for the Fatigue Assessment of Welded Structures by Notch Stress Analysis: IIW-2006-09, Woodhead Publishing, 2012.
[36] C.M. Sonsino, W. Fricke, F. De Bruyne, A. Hoppe, A. Ahmadi, G. Zhang, Notch stress concepts for the fatigue assessment of welded joints–background and applications, Int. J. Fatigue 34 (1) (2012) 2–16, https://doi.org/10.1016/j.ijfatigue.2010.04.011.
[37] W. Fricke, IIW guideline for the assessment of weld root fatigue, Welding World 57 (2013) 753–791, https://doi.org/10.1007/s40194-013-0066-y.
[38] J. Schijve, Fatigue predictions of welded joints and the effective notch stress concept, Int. J. Fatigue 45 (2012) 31–38, https://doi.org/10.1016/j.ijfatigue.2012.06.016.
[39] D. Radaj, C.M. Sonsino, W. Fricke, Fatigue Assessment of Welded Joints by Local Approaches, Woodhead publishing, 2006.
[40] K. Tateishi, N. Soda, T. Hanji, M. Shimizu, Displacement based fatigue strength evaluation for root failure in fillet weld joints, J. JSCE, Ser. A1 71 (3) (2015) 315–326 (in Japanese), https://doi.org/10.2208/jscejseee.71.315.
[41] A.R.G. Azad, K. Kreitman, M. Engelhardt, T. Helwig, E. Williamson, Large-scale fatigue testing of post-installed shear connectors in partially-composite bridge girders, J. Constr. Steel Res. 161 (2019) 57–69, https://doi.org/10.1016/j.jcsr.2019.06.007.